Thermal Science and Engineering Progress 48 (2024) 102352

Contents lists available at ScienceDirect

Thermal Science and Engineering Progress

journal homepage: www.sciencedirect.com/journal/thermal-science-and-engineering-progress

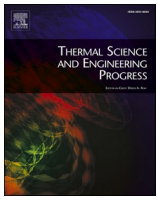

Investigating heat transmission in a wellbore for Low-Temperature, Open-Loop geothermal systems

Christopher S. Brown *, Gioia Falcone

James Watt School of Engineering, University of Glasgow, Glasgow G12 8QQ, UK

ARTICLE INFO

Keywords:
Geothermal
Geothermal wellbore
Numerical modelling
OpenGeoSys
Production well

ABSTRACT

Heat transfer processes in geothermal wellbores are an essential component to overall system performance, but can be overlooked in subsurface modelling studies that tend to focus on reservoir response. This study addresses heat transfer in the wellbore through a comprehensive modelling study of 10 different parameters on OpenGeoSys software designed to evaluate heat losses during open-loop production conditions for typical low-temperature (<100 °C) single phase geothermal systems. Models were set-up to focus on wellbore effects only, using a single production well with constant fluid inlet temperature boundary condition. Results indicate that under base case conditions for a 2-km deep well surrounded by rock formations with a thermal conductivity of 2.5 W/(m.K) and bottom-hole temperature of 60 °C, the difference in inlet (reservoir) and production (wellhead) temperature at the end of a 40-year production period is 2.06 °C. This corresponds to minimum heat losses into the surrounding formations of −63.3 W/m, which is ~ 7 % of the thermal power recorded at the wellhead (assuming a rejection temperature of 30 °C) and a 3.4 % difference to bottom-hole temperature. These losses in heat can be significant, particularly when in combination with surface losses through the heat exchanger or in the reservoir through thermal breakthrough. Wellbore insulation can reduce losses, but it would appear this only impacts the short-term. Wellbore performance can also be improved, with heat losses minimized, when developing wells above the reservoir interval in low thermal conductivity rock with high geothermal gradients.

1. Introduction

Geothermal developments can contribute to the decarbonisation of heat globally by providing energy for power generation, space heating/cooling or direct-heat use applications. Open-loop geothermal systems typically consist of a subsurface reservoir (or enhanced/engineered geothermal system in the subsurface), production/injection wellbores and surface infrastructure to harness the thermal energy. Whilst much research has been undertaken on the various components of a geothermal system, including heat loss in a wellbore, few have comprehensively investigated heat transmission from the wellbore under transient conditions for a low-temperature, single phase system, with the purpose of identifying optimum parameters to minimise heat losses under different geological and engineering conditions.

Initial work on heat transfer in a wellbore was undertaken by Ramey Jr [32], who developed a transient analytical solution which accounted for thermal resistance within a wellbore, with various modifications to the solution implemented since (e.g., [37,29]). These solutions are useful for finding the temperature of a fluid within a well as a function of time and depth, but can provide erroneous results for short-term simulations where temperature is significantly overestimated [18]. Although for long-term simulations such errors would have negligible impact on the overall performance.

Many have evaluated the performance of heat transfer from a wellbore in a geothermal system. Tantuoyir [41] studied the impact of insulation and other parameters within a high temperature geothermal system with a steady-state model developed on WELLCAT^{TM} software. They found that insulation and high flow rates reduce heat loss, whilst cement thermal conductivity is important in non-insulated wells. Wardana et al. [42] developed a model to analyse the performance of a steam dominated geothermal system; showing heat loss to be minimal (<2 W/m). Kanev et al. [22] also investigated high temperature systems, analysing the short-term (<1000 days) heat transfer within a geothermal wellbore. They established heat transfer effects are important when the elapsed time or flow rate is small. Kutun et al. [26] also developed a model; they identified that with increasing flow rates stabilisation times for production temperature are reduced (i.e., for the system to reach a quasi-steady state). Some have analysed low-temperature systems using analytical solutions but focus on limited

* Corresponding author.
E-mail address: christopher.brown@glasgow.ac.uk (C.S. Brown).

https://doi.org/10.1016/j.tsep.2023.102352
Received 19 October 2023; Received in revised form 18 December 2023; Accepted 19 December 2023
Available online 22 December 2023

Nomenclature

c	*specific heat capacity*
$\varnothing$	*porosity*
ρ	*density*
H	*heat source*
T	*temperature*
Φ	*thermal resistance*
Λ	*hydrodynamic dispersion tensor*
λ	*thermal conductivity*

Subscripts

s	*solid*
w	*groundwater*
g	*grout*
f	*fluid in the pipe*

parameterisation and steady-state solutions for data matching (e.g., [24]). Furthermore, analytical, and numerical solutions have been utilised for estimating static, steady-state and transient temperature distributions with specific application for the oil and gas industry (e.g., see [19], among others) or for during drilling of boreholes (e.g., see [27,43]).

Several numerical solutions have also been developed for geothermal wellbores: i) some utilise the drift flux method, such as T2Well (see [46,39,30,31,17]), ii) others adopt a full discretisation of the wellbore and surrounding rock, such as ANSYS-FLUENT (e.g., [1]), or TOUGH2 [34] and iii) others use a 'Dual-continuum' approach, including OpenGeoSys (OGS), COMSOL and models developed on MATLAB (e.g., [35,11,12,6,2,25]). Models that utilise the 'Dual-continuum' approach are typically derived following work from Al-Khoury et al. [3] and Al-Khoury and Bonnier [4] who originally developed the method for shallow geothermal systems. Other software, such as FEFLOW, also have the capabilities of modelling analytical, full discretisation and 'Dual-continuum' approaches (e.g., see [14,15]). The benefit and popularity of the 'Dual-continuum' approach stems from the fact it saves computational time by modelling the wellbore components in 1D, integrated within a 3D geological medium. This can, therefore, be used in conjunction with reservoir models. However, it should be noted such models can have limitations (such as inability to model varying casing strings).

As discussed, many numerical and analytical modelling approaches exist for both steady-state and transient simulations; this study aims to build on past literature by providing a comprehensive investigation into the impact of 10 geological and engineering parameters through transient numerical modelling studies of low-temperature, single phase systems (i.e., <100 °C), focusing on limiting heat-loss through the wellbore from bottomhole temperature to the wellhead. Therefore, the purpose of this paper is to evaluate heat loss, using OGS software, within a typical production geothermal wellbore under low-temperature single phase conditions, where it is assumed well completion is based on idealised self-discharging wells (i.e., artesian – for instance, similar to the conditions in Oradea, Romania [34]. It is worth noting however, that many low-temperature, single phase systems may require artificial lift (e.g., [45]). While many models could be adopted for this study, OGS was chosen as it has the capability to be coupled to reservoir models, but it also has the benefit of having relatively fast computational times due to the adoption of the 'Dual-continuum' method. Therefore, this paper provides analysis over the lifetime of a geothermal production wellbore under 10 different parameters to understand the impact on thermal performance.

2. Methods

2.1. Governing equations

OGS software was used to model heat transmission in the wellbore; fluid flows from the reservoir, through the central pipe which is surrounded by cement (Fig. 1) cooling through conductive heat transfer through the borehole wall, reducing in temperature as the fluid approaches the surface level. In reality, multiple casing strings would be used in development and well design; however, in this case a simplified, single diameter cased section was modelled. This is due to limitations within the software. The 'Dual-continuum' approach was implemented, using 1D line elements for the borehole and 3D elements to model the subsurface geology. The governing equations for the borehole design in this study are after Chen et al. [12]. For further information on OGS design and implementation see Kolditz et al. [23], among others. Groundwater flow was neglected as other studies on wellbores (albeit closed-loop) have shown it to have limited impact [11,9]. The surrounding rocks were modelled to account for conductive heat flux:

$$\frac{\partial T_s}{\partial t}[\varnothing\rho_w c_w + (1-\varnothing)\rho_s c_s] - \nabla \bullet (\Lambda_s \bullet \nabla T_s) = H_s \tag{1}$$

where T_s is the temperature of the rock, t is time, $\varnothing$ is porosity, ρ is the density, c is the specific heat capacity, Λ_s is the hydrodynamic dispersion tensor and H_s is a source or sink. The subscripts w and s denote the values for groundwater and the solid rock.

Heat flux on the boundary between the surrounding rock mass and the wellbore is described as:

$$q_{nT_s} = -\Phi_{gs}(T_g - T_s) \tag{2}$$

where Φ_{gs} is the thermal resistance between rock and cementitious grout, T_g is the temperature of the cementitious grout in the wellbore. Heat transport within the cemented section of the borehole occurs through heat conduction:

$$\frac{\partial T_g}{\partial t}\left[(1-\varnothing)\rho_g c_g\right] - \nabla \bullet \left((1-\varnothing)\lambda_g \bullet \nabla T_g\right) = H_g \tag{3}$$

with heat flux on the boundaries dominated by thermal resistance between the solid rock and the fluid within the borehole:

$$q_{nT_g} = -\Phi_{gs}(T_s - T_g) - \Phi_{fg}(T_f - T_g) \tag{4}$$

where Φ_{fg} is the thermal resistance between fluid and cement, T_f is the temperature of the fluid in the wellbore.

Fluid flow within the central pipe occurs through advection:

$$\frac{\partial T_f}{\partial t}\rho_f c_f + \rho_f c_f v_f \bullet \nabla T_f - \nabla \bullet \left(\Lambda_f \bullet \nabla T_f\right) = H_f \tag{5}$$

where heat transfer on the boundary with the cement occurs as:

$$q_{nT_f} = -\Phi_{fg}\left(T_g - T_f\right) \tag{6}$$

and the subscript f is for the fluid, v_f is for the velocity of the fluid (calculated and implemented as an average across the system from the mass flow rate/pipe area). For further information on calculating borehole resistances see Diersch et al. [14,15] and Diersch [16].

2.2. Parameters, boundary and initial conditions

The parameters in this section were chosen to represent those in a typical sedimentary succession for low-temperature, hydrothermal systems. Without adopting a specific case study, they are designed to have general application for low-temperature geothermal developments. The geothermal gradient was set-up to increase linearly by 25 °C/km, with the surface temperature set at 10 °C (Fig. 2). This, in combination with the base case thermal conductivity (2.5 W/(m.K)), is similar to the average heat flow for the UK (excluding high heat flow granites) [33]

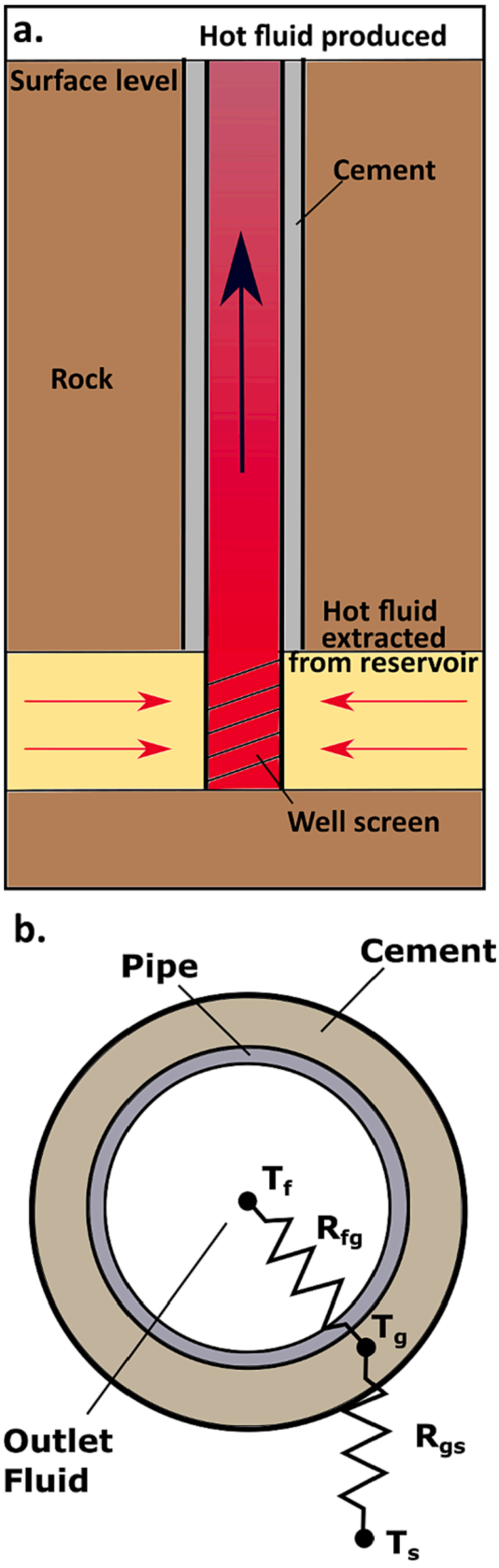

Fig. 1. (a) Schematic of a producing well in a conventional geothermal system targeting a hot sedimentary aquifer (modified from [8]). (b) Cross section through the wellbore, with thermal resistance network.

and Europe [28]. At the start of the simulation under the initial conditions, the fluid and cement within the borehole were set to equal the ground temperature (i.e., increasing with the natural geothermal gradient).

Boundary conditions were established as i) fixed Dirichlet boundary condition at the surface of 10 °C, ii) Neumann no-flow lateral boundaries, iii) Neumann boundary with constant heat flow calculated from the geothermal gradient and rock thermal conductivity applied to the basal boundary, and iv) a constant inlet temperature of the reservoir fluid into the wellbore from the base of the model. This condition was applied to normalise results and highlight the impact of wellbore effects only on a production well; therefore, the model does not account for thermal interference between producers and injectors (i.e., there is no thermal breakthrough). In practice there would be a cooling effect within the reservoir caused by the re-injection of cool water. Lateral boundaries were designed to be far enough away from the borehole such that no boundary interference occurred for the course of the simulation. The domain was extended by 500 m x 500 m (x,y) whilst the length of the borehole and depth of the model (z) was 2 km (Fig. 2).

Base case model parameters are listed in Table 1.. A range of parameters were modelled to understand the impact of typical parameters that might be encountered in a low-temperature geothermal system: borehole depth (1–3 km), borehole radius (0.1778–0.254 m (7–10 in.)), cement thermal conductivity (1–5 W/(m.K)), inner pipe diameter (0.15–0.19 m (5.9–7.5 in.)), fluid flow rate (10–40 l/s), pipe thermal conductivity (0.5 to 50 W/(m.K)), reservoir (inlet) temperature (60–95 °C), rock thermal conductivity (1–4.5 W/(m.K)), geothermal gradient (20–40 °C/km) and volumetric heat capacity (1.8–2.4 MJ/(K m^3)). These were simulated for a time period of 40 years to evaluate their impact on performance over the lifetime of the system., which was considered to be an absolute maximum.

2.3. Model benchmarking

A series of solutions were simulated to compare the performance of OGS to other wellbore simulators. These included i) the analytical solution by Ramey Jr [32] – obtained from Chen and Shao [13] and ii) a numerical model developed by Brown et al. [6]. A 40-year simulation was undertaken using the parameters outlined in Table 1. This was somewhat simplified by using the average undisturbed ground temperature for the initial conditions (35 °C).

The outlet temperature rapidly warmed across all models in the first few months due to the higher inlet temperature of 60 °C, before showing a gradual increase after this period with the outlet temperatures asymptotic to the inlet temperature (Fig. 3a). The models provided good agreement with end temperatures within 0.3 °C of each other, corresponding to a maximum percentage difference of 0.3 % to OGS (Fig. 3a). Ramey's solution provides the highest estimate with an end production temperature recorded as 58.16 °C, whereas the model by Brown et al. [6] provides an end temperature value of 57.86 °C and OGS produces an end production value of 57.99 °C. These result in differences between wellhead and inlet (reservoir) temperatures of 1.84 °C, 2.14 °C and 2.01 °C, respectively. The solutions provide minimal discrepancy in the long term; however, there is minor discrepancy in the short term (<2 days). This is consistent with other literature which suggests the solution provided by Ramey can over-predict temperatures in shorter periods [18], or observes differences to other solutions [12]. Nonetheless, the long-term results provide confidence that the solution on OGS converges to give accurate results, particularly when looking at the final vertical profile of fluid temperature in the wellbore where the difference in the models was < 0.3 °C over the 2 km borehole (Fig. 3b).

2.4. Evaluation of performance

It is important to consider the performance of the system by evaluating heat losses. In this study, heat losses (q) were evaluated as follows:

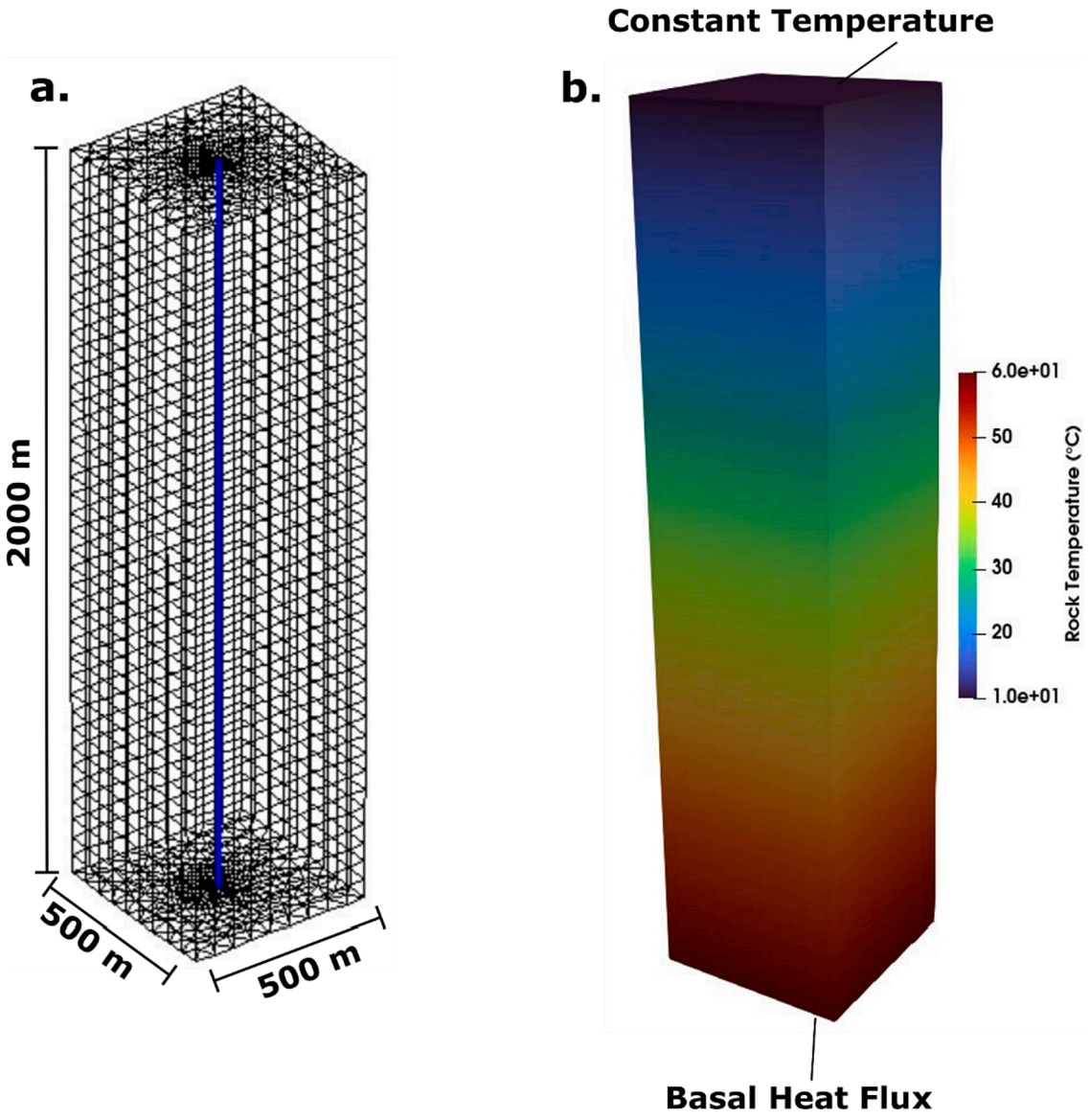

Fig. 2. (a) Example mesh and (b) Model static set up for the base case scenario.

Table 1
Base case parameters. Note water viscosity and density are calculated based on the inlet as the reference temperature (i.e., at 60 °C). Parameters adopted after Banks [5], Rollin [33], Younger et al. [44] and Kolo et al. [25].

Parameter	Value	Units
Borehole diameter	216	mm
Inner pipe diameter	177.8	mm
Pipe thickness	0.008	m
Pipe thermal conductivity	10	W/(m.K)
Borehole length	2000	m
Ground thermal conductivity	2.5	W/(m.K)
Ground volumetric heat capacity	2×10^6	J/(K m^3)
Water flow rate	15	l/s
Water density	980	kg/m^3
Water volumetric heat capacity	4.095×10^6	J/(K m^3)
Water thermal conductivity	0.59	W/(m.K)
Water viscosity	47×10^{-4}	kg/(m s)
Basal heat flow	62.5	mWm^{-2}
Geothermal gradient	25	°C/km
Surface temperature	10	°C
Inlet temperature	60	°C
Cement thermal conductivity	1.05	W/(m.K)
Cement volumetric heat capacity	1.2×10^6	J/(K m^3)

$$q = \frac{mc_w\rho_w(T_{in} - T_{out})}{L} \quad (7)$$

where m is the mass flow rate, T_{in} is the inlet temperature from the reservoir, T_{out} is the production temperature and L is the length of the well. Other parameters are listed in section 2.1. Using equation (7), the value for specific heat rejected into the formation (W/m) is always negative to indicate heat leaving the borehole.

3. Results

3.1. Temporal thermal evolution of the system

The temperature at the wellhead rapidly increases in the first few days, as under static conditions temperature increases with depth (Figs. 4, 5 and 6). After the first few days of production, change in temperature at the wellhead is minimal as production temperature reaches a near quasi-steady state as the local thermal field reaches a near equilibrium heat flow in response to the borehole (Figs. 4 and 5). At the end of the simulation the production temperature was recorded at 57.94 °C (Fig. 4), indicating heat losses in the wellbore of 2.06 °C or a heat rate of −63.3 W/m. Whilst there are some heat losses, the overall

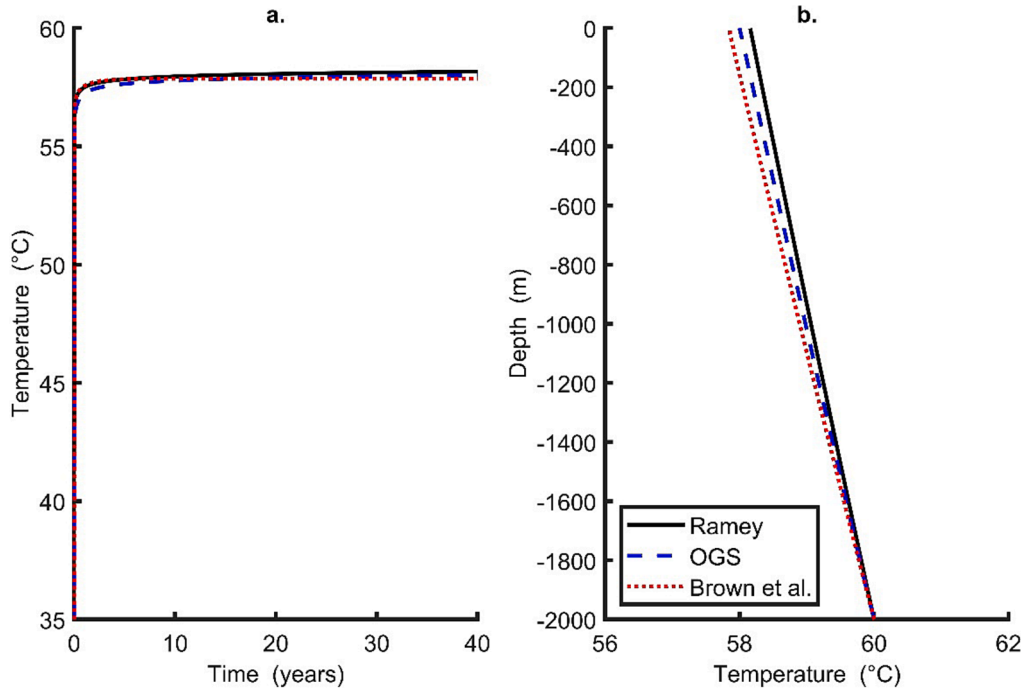

Fig. 3. (a) Outlet temperature versus time and (b) modelled temperature recorded at the end of the simulation across the vertical profile of fluid within the wellbore.

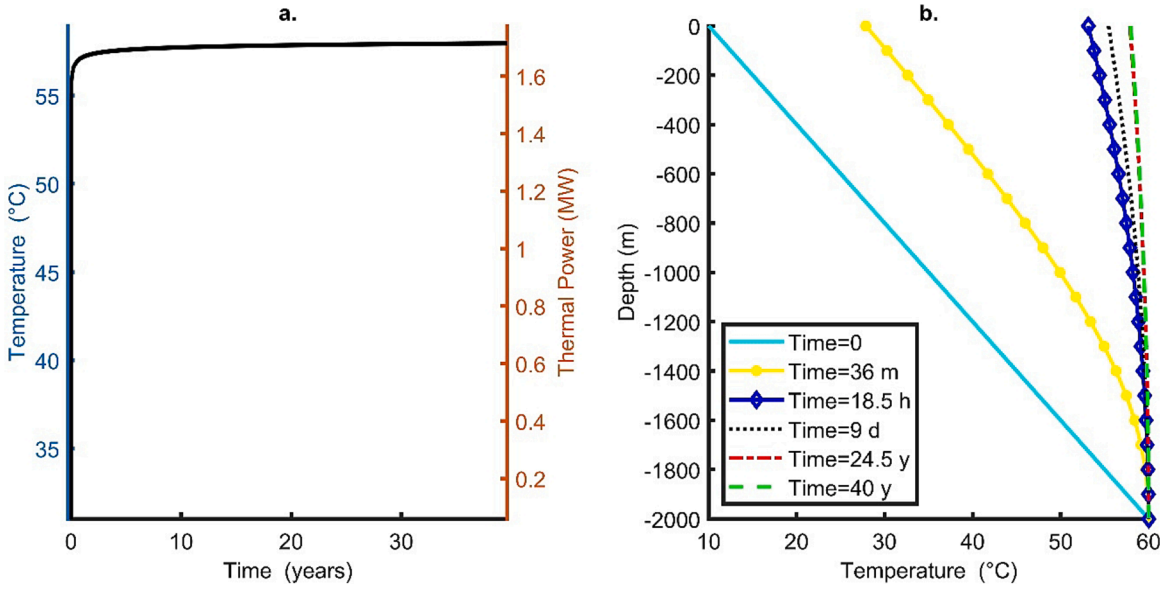

Fig. 4. (a) Outlet temperature and thermal power recorded at the wellhead versus time. (b) Varying time vertical profiles of fluid temperature in the wellbore. Note m = minute, h = hour, d = day and y = year.

thermal power at the wellhead was recorded at 1.72 MW assuming a rejection temperature of 30 °C. This is 127 kW less than if 60 °C was used as the output and consequently, would give significant differences in total energy produced over the lifetime of a system. The heat losses of −63.3 W/m (or −127 kW) is equivalent to 7 % of the thermal power and was recorded at the end of the simulation providing the lowest heat losses over time in the wellbore (Fig. 7). For instance, at 1-year heat losses were recorded as over 10 % in comparison to the thermal power; however, after this there is a steady decline in heat transfer as the surrounding formations warm.

The large heat losses into the subsurface from the wellbore result in radial thermal propagation of heat away (Figs. 5 and 8). More heat is lost at the top of the borehole due to a greater difference in temperature between the wellbore and the surrounding rock (Fig. 8a). This is highlighted when comparing 100 m depth to 1900 m. The thermal radius for both levels at the end of the simulation was recorded to within 0.1 °C of static conditions at 125 m and 65 m, respectively. The thermal propagation of heat in the nearby thermal field can also be observed to increase with time (Fig. 8b) where it increases to a maximum radial thermal propagation of 110 m (for 1000 m depth).

3.2. *Influence of geological parameters*

Several geological parameters, including the geothermal gradient, volumetric heat capacity, rock thermal conductivity and inlet temperature (i.e., reservoir temperature), were modelled to investigate how

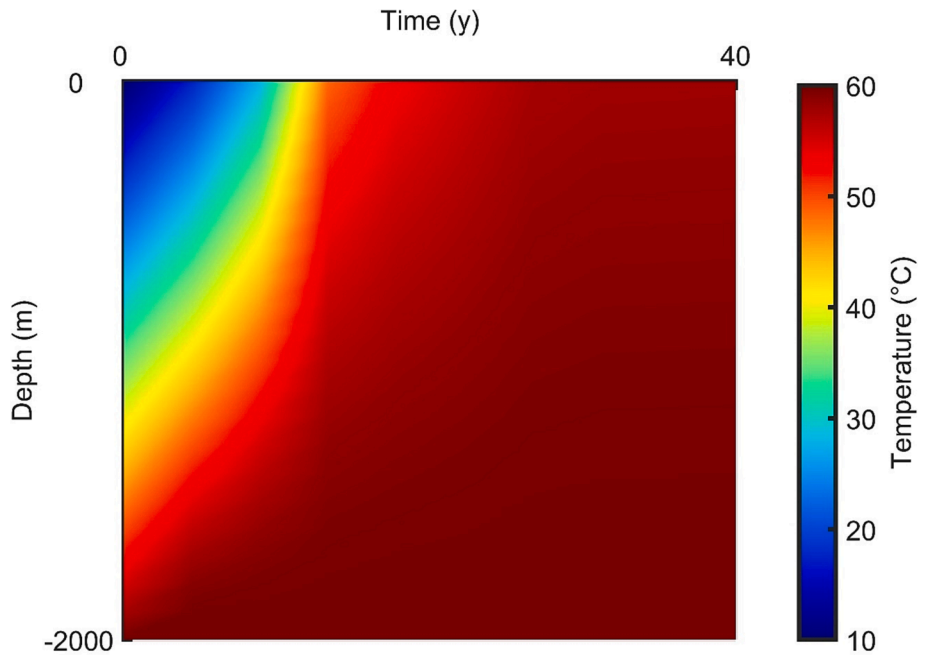

Fig. 5. Temperature of fluid in the wellbore varying with time. Note the time scale is not uniform.

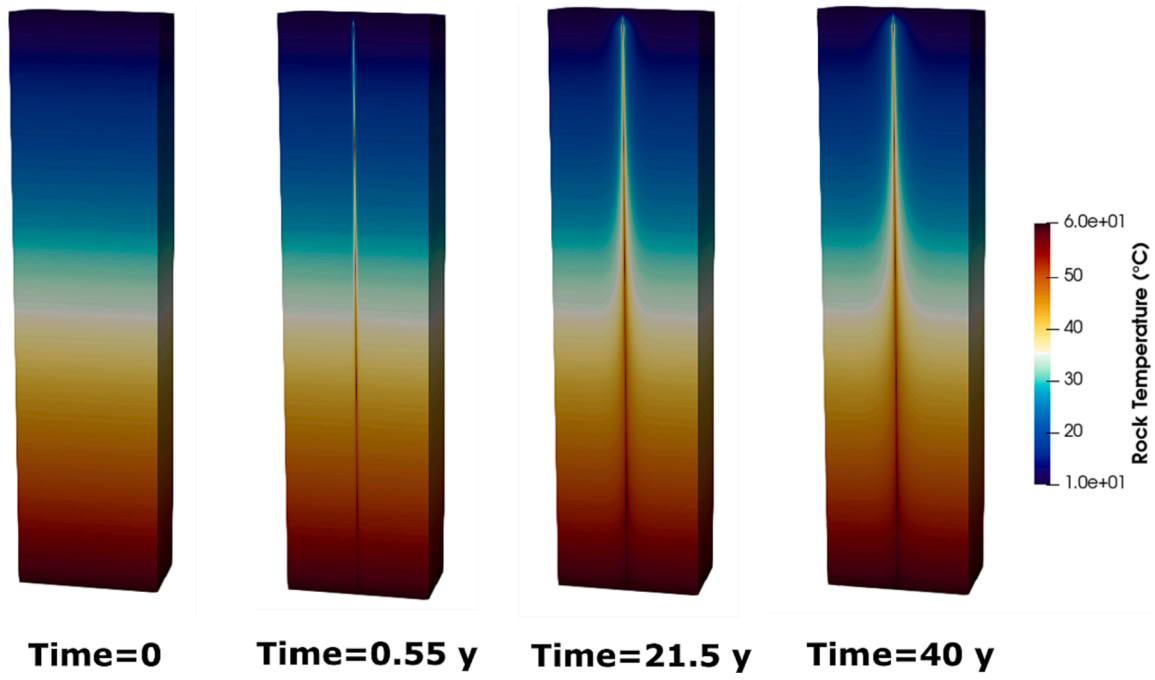

Fig. 6. 3D visualisation of heat flow around the borehole for varying times.

they impacted production and heat losses in a geothermal wellbore. The initial geothermal gradient under static conditions is essential to determine the production temperature and, thus, thermal power for a system. Whilst it is beneficial to have a greater geothermal gradient as it has a positive linear relationship with production temperature and thermal power, it does create greater heat losses from the wellbore to the surrounding formation (Fig. 9a). This is due to the fact there is an increased maximum temperature differential. The minimum thermal gradient of 20 °C corresponds to heat losses of −50.7 W/m, whilst for the maximum thermal gradient modelled of 40 °C the heat losses were −101 W/m. These correspond to a difference in 1.64 °C and 3.35 °C between the inlet and wellhead temperature, respectively.

Volumetric heat capacity was also varied between the typical range observed for rocks in the subsurface (e.g., [5]), yet had a minimal impact on production temperature and heat rate out of the wellbore. The range in end production temperature observed was 0.04 °C and heat rate was 1.3 W/m. In contrast, the other thermo-physical rock parameter modelled (rock thermal conductivity) had a more significant impact. For rock thermal conductivities, a range from 1 to 4.5 W/(mK) was modelled, a linear negative relationship was observed for both end temperature and heat rate. The minimum and maximum heat losses were recorded at the end of the simulation of −28.5 W/m and −103 W/m. The minimum and maximum recorded end wellhead temperatures were thus 59.1 °C and 56.6 °C, respectively.

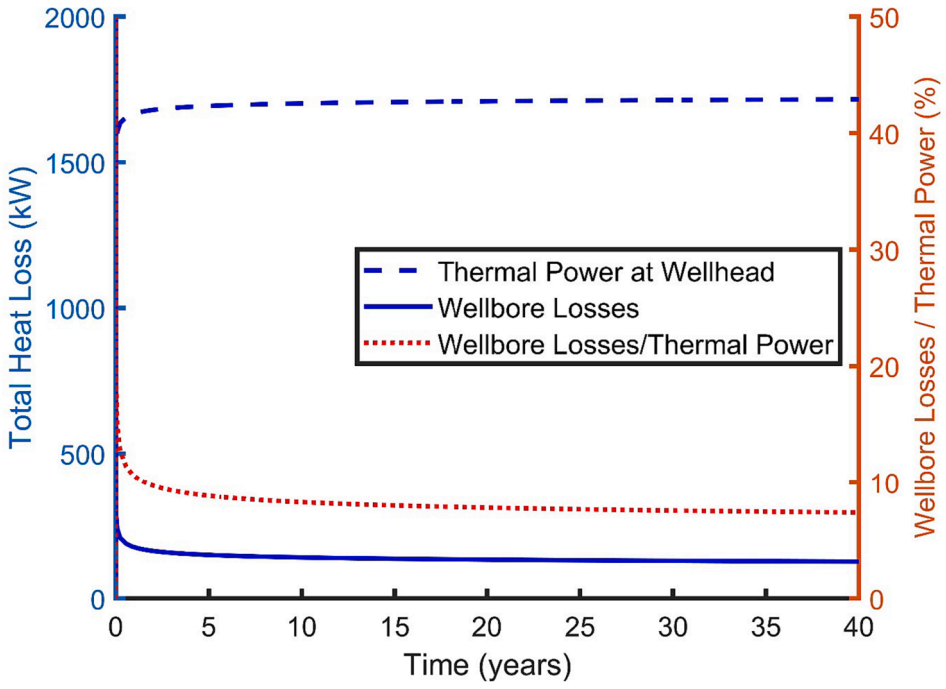

Fig. 7. Thermal power at the wellhead, the wellbore heat losses and ratio of losses to thermal power plotted over time.

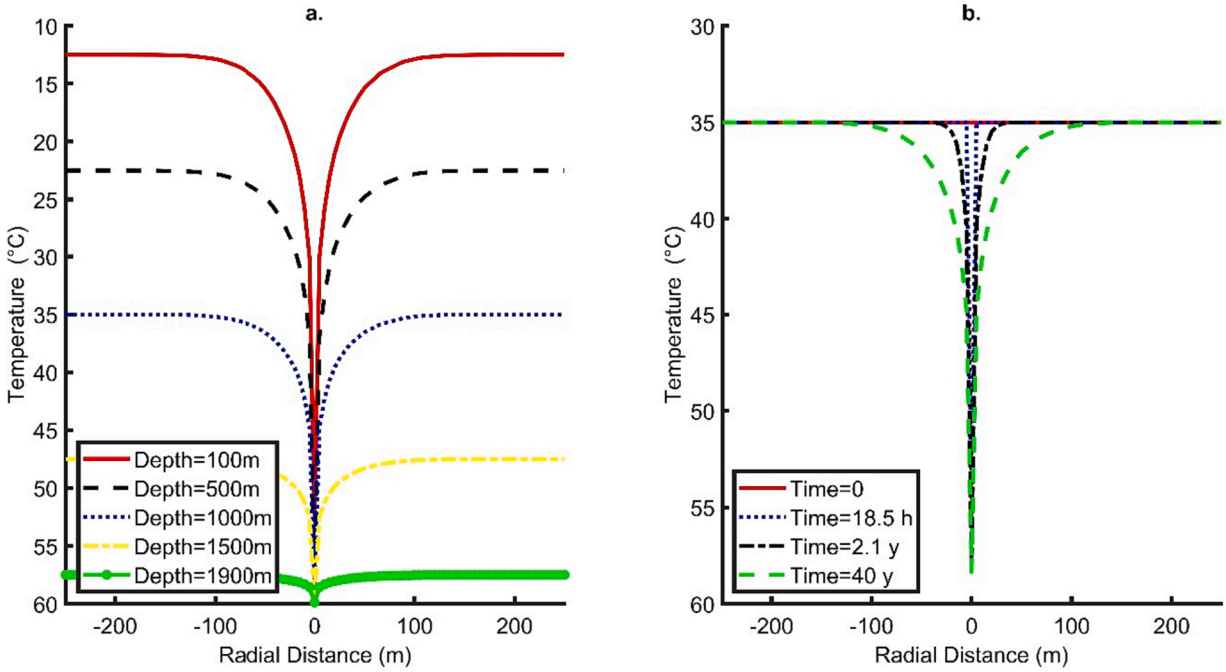

Fig. 8. (a) Temperature in the rock around the borehole (located at point 0). (b) Varying time radial temperature in the rock at 1000 m for varying time intervals. Note h = hour and y = year.

Finally, inlet (or assumed reservoir) temperature was also modelled as a separate entity. In reality, this would be dictated by the geothermal gradient, depth, reservoir conditions and geothermal system. Nevertheless, a range of conditions were modelled and the results were similar to that of varying the geothermal gradient. An increase in inlet temperature resulted in a linear relationship with production temperature and thermal power, but heat losses increased with thermal power. The maximum inlet temperature measured (95 °C) produced an end production temperature of 90.05 °C and heat losses of −149 W/m. Therefore, engineering conditions could be used to establish optimal conditions to minimize heat losses.

When considering the major impacting factors (initial geothermal gradient, which can account for the inlet temperature, and rock thermal conductivity) maximum production temperatures and heat losses can be established (Fig. 10); greater thermal powers are reached for higher geothermal gradients, but heat loss can be significantly minimized when drilling in lower rock thermal conductivity. This is due to the rock insulating the borehole and minimizing heat transfer out and into the subsurface. In contrast, higher rock thermal conductivities maximize heat transfer into the rock.

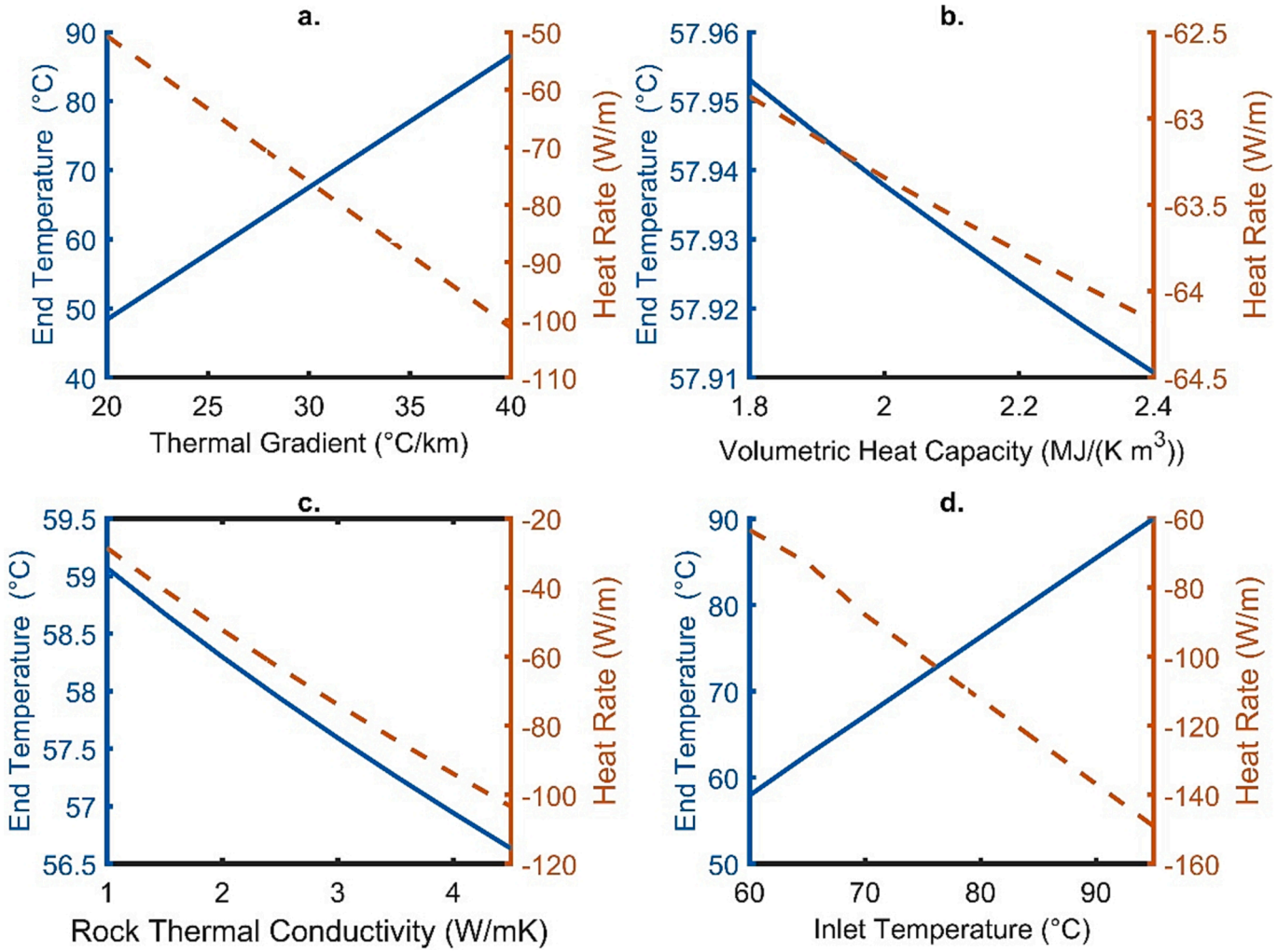

Fig. 9. Production temperature at the end of the simulation and corresponding heat losses from the wellbore for a variety of parameters including (a) geothermal gradient, (b) volumetric heat capacity, (c) rock thermal conductivity and (d) inlet temperature.

3.3. Influence of engineering parameters

A range of engineering parameters were also modelled including depth, borehole diameter, inner pipe diameter, pipe thermal conductivity, cement thermal conductivity and flow rate (Figs. 11 and 12). The depth of the wellbore has a strong influence on the end production temperature and also the heat rate (Fig. 11a). As depth increases, this leads to greater inlet temperatures into the borehole. Therefore, there is a larger difference in temperatures and more heat transfer out of the wellbore and into the confining rocks. There is also a longer transit time at depth and more heat can be lost. However, in contrast the production temperature and thermal power increases with depth. As a result, the minimum production temperature experienced was 34.5 °C for a 1 km deep borehole and a maximum production temperature of 80.4 °C for a 3 km wellbore.

Other parameters such as borehole diameter, inner pipe diameter, cement thermal conductivity and pipe thermal conductivity all have minimal impact on heat losses and end production temperature (Fig. 11b and 12). If a system is operating intermittently; however, these parameters could have more of an impact, as studies have shown wellbore material can influence the short term [36] but if using constant base load production it is likely they will not impact a system significantly. Indeed, in this study for the highest thermal conductivity of cement modelled (5 W/(mK)) slightly higher losses were recorded in the first year, which corresponded to 12 % of the thermal power. The final parameter modelled was flow rate. Interestingly the variation in heat rate was minimal due to the decreasing flow rate corresponding to greater differences in outlet temperature in comparison to inlet temperature, but this balances against the increase in fluid (and energy) produced (Fig. 12d).

4. Discussions

4.1. Impact of key parameters

This study has highlighted that heat transmission in a wellbore can play an integral role in determining heat losses, production temperature and also the achievable thermal power (thus the total energy produced from a low-temperature, single phase geothermal system). The most important parameters appear to be rock thermal conductivity, geothermal gradient, inlet (reservoir) temperature, depth and flow rate. In many scenarios, these parameters may be predetermined by the local in-situ properties of the subsurface; however, during well planning if the geology is well constrained then losses could be somewhat minimised using directional drilling (although this could significantly increase costs). The latter parameter (i.e., flow rate) may be determined by the hydraulic characteristics of the reservoir, but it would appear it mainly impacts achievable thermal power and production temperature, rather than the heat losses from the wellbore. Therefore, it is best to maximise this when exploiting conventional geothermal systems. Although, on the

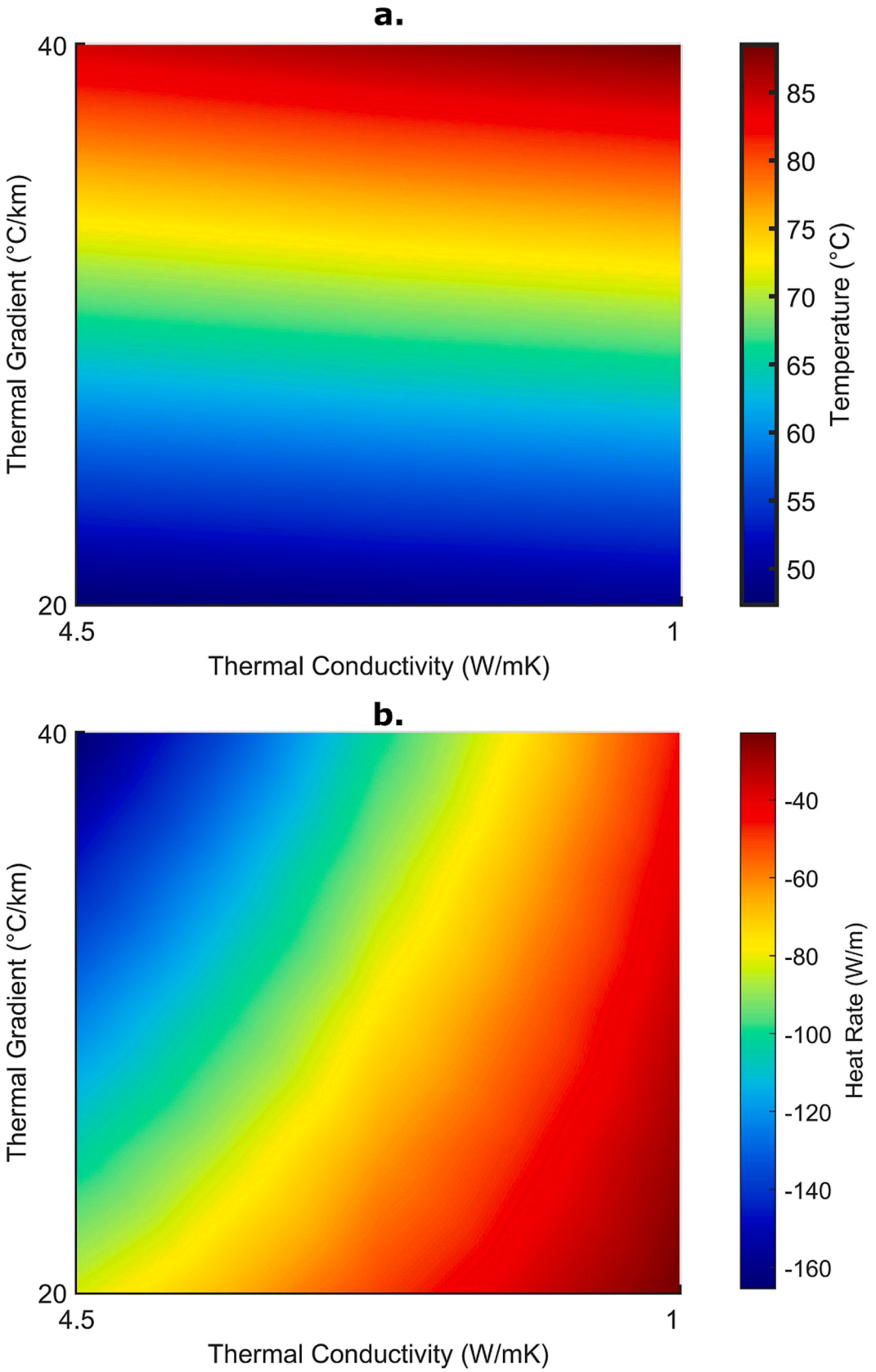

Fig. 10. Production temperature at the end of the simulation (a) and corresponding heat losses from the wellbore (b) for thermal gradient plotted against rock thermal conductivity.

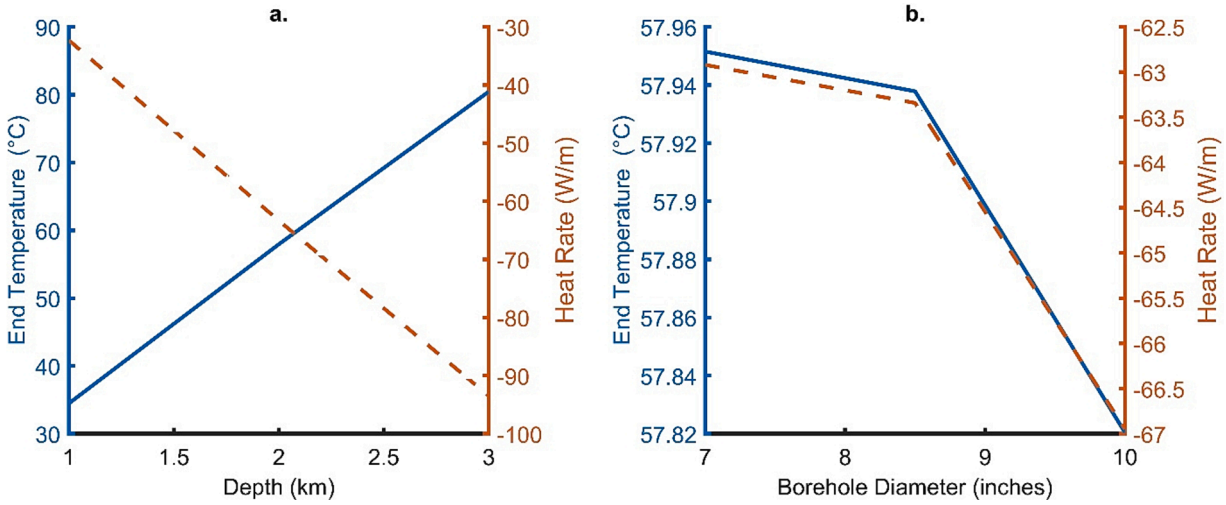

Fig. 11. Production temperature at the end of the simulation and corresponding heat losses from the wellbore for a variety of parameters including (a) depth and (b) borehole diameter.

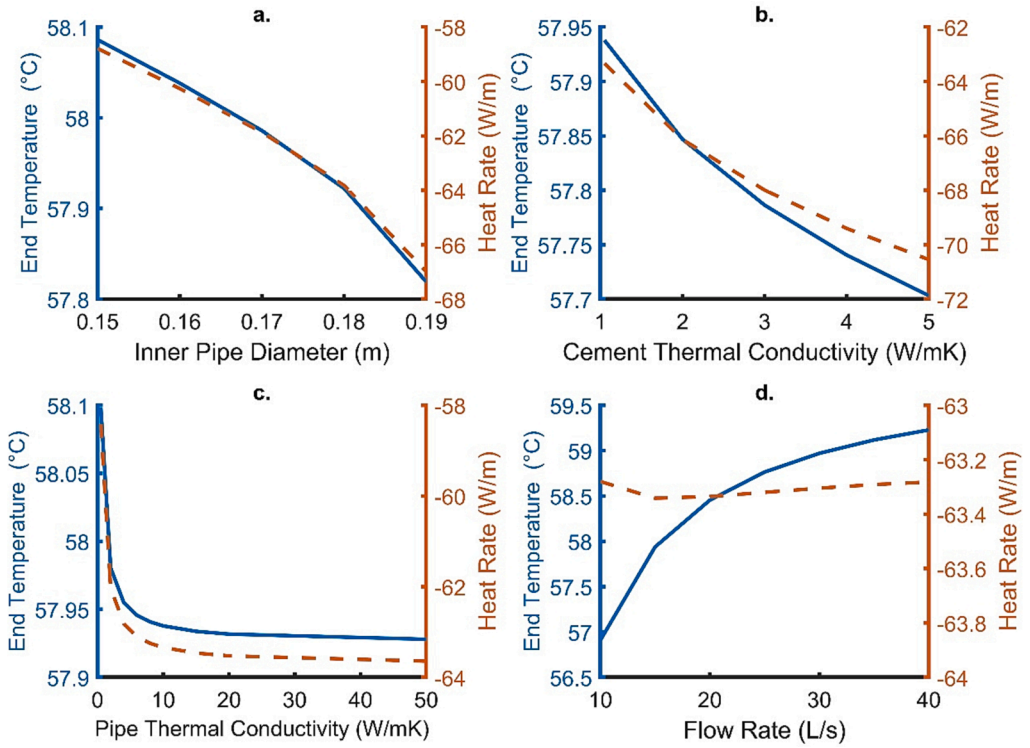

Fig. 12. Production temperature at the end of the simulation and corresponding heat losses from the wellbore for a variety of parameters including (a) inner pipe diameter, (b) cement thermal conductivity, (c) pipe thermal conductivity and (d) flow rate.

other hand, if an electric submersible pump is required for any part of operations, then there will be greater parasitic losses. Impacts of variable operation (i.e., intermittency) could also be investigated further as it was shown that thermal insulation of the wellbore only impacts the short term. Therefore, future work should look to address some of the modelling limitations such as multiple casing strings, hydraulic losses, and intermittent operation.

4.2. Comparison of results with literature

When comparing the results of this study to other literature investigating heat transfer within a deep geothermal wellbore some conclusions can be shared. It would appear for low-temperature (<100 °C) geothermal systems that the quasi-steady state production temperature and nearby heat flow field is reached very quickly. Between the end of the first and last years of simulation the difference in production (wellhead) temperature was less than 1 °C (for the initial base case). This is in agreement with Rosca [34], among others, who also suggest that steady-state conditions occur rapidly when using a constant flow rate for operation. Although the impact of thermal breakthrough within the reservoir could affect the validity of such assumptions. The study does show contrasting results to other authors who have modelled heat losses encountered in wellbores in other types of geothermal systems. For instance, steam dominated systems show far lower heat losses

within the wellbore [42].

4.3. Comparison of modelling with and without geothermal gradient

Interestingly, it would appear that modelling the geothermal gradient or a uniform temperature of the rock has minimal impact on the overall results. This is due to the fact that the total available energy within the domain is the same in both scenarios and thus, does not impact long-term performance when assessing heat transfer from a geothermal wellbore. It may, however, have more impact on short-term or intermittent production conditions. This has further connotations for real system analysis and modelling of the wellbore; it indicates model simplifications can hold for long-term scenarios with constant production conditions. It also suggests that the results may be applicable for horizontal (or directional geothermal wellbores).

4.4. Wider applications of results

The findings of this work also have applications when exploiting unconventional resources, such as using large closed-loop systems in a U-type heat exchanger (e.g., [20,21]), or using deep coaxial borehole heat exchangers (e.g., [10]) when assessing heat losses to the surrounding subsurface rock. It has shown that the engineering of the system generally has a reduced impact on the heat losses than the local geology. Although it is worth noting coaxial borehole heat exchangers and large scale closed-loop systems have more engineering complexity than that of a single producing well which was modelled in this work. There are other limitations of this study that should be investigated in future work, these include; understanding the impact of an electric submersible pump and different casing strings.

5. Conclusions

In this study, a comprehensive analysis of heat transmission in low-temperature geothermal wellbores was undertaken using finite-element, numerical models; OpenGeoSys software was utilised to simulate heat rate in a wellbore over a 40-year lifetime. Initial benchmarking was undertaken to test the model suitability in comparison to other solutions, including an analytical solution [32] and a finite-difference numerical model by Brown et al. [6]. The solutions provided little discrepancy with production temperature within 0.3 °C of each other at the end of the solution. Following initial benchmarking a range of parameters were modelled to investigate heat rate from a geothermal wellbore. The key conclusions were:

- Heat losses from a wellbore can reduce overall system performance, particularly when in consideration with other losses at surface level through inefficiencies during heat exchange [7] or in the subsurface reservoir associated to cooling from reinjection and thermal breakthrough effects on the production well (e.g., [38,40]). Combining these losses will significantly limit the lifetime.
- Under initial base case parameters the difference in inlet and production temperature at the end of a 40 year simulation from a 2 km well was 2.06 °C, corresponding to heat losses of −63.3 W/m. This corresponds to a minimum of 7 % of the total thermal power produced (assuming a rejection temperature of 30 °C). Heat losses are greater in the first few years of operation before the system reaches a steady state.
- Wellbore insulation does not play a significant role, except in early production. For the highest thermal conductivity cement (5 W/(mK)) heat losses corresponding to 12 % of the thermal power were recorded in the first year, whilst for the lowest thermal conductivity 10 % was recorded. This could play more of a role in systems which require intermittent operation.
- Geological parameters such as initial geothermal gradient, inlet (reservoir temperature) and thermal conductivity have a significant impact on heat transfer from a wellbore, while the influence of volumetric heat capacity of the rock on thermal losses is minimal.
- Heat loss is greatest for high geothermal gradient systems and high rock thermal conductivities.
- Engineering parameters such as depth and flow rate impact the maximum production temperatures. However, only depth has a major impact on heat losses. Borehole diameter, inner pipe diameter, cement thermal conductivity, pipe thermal conductivity and flow rate play a small role in heat transmission from the wellbore to the surrounding rocks.
- When modelling a well with and without the geothermal gradient the impact appears to be minimal. Production temperatures recorded at the end of the simulation were recorded within 0.05 °C of each other.

Declaration of competing interest

The authors declare that they have no known competing financial interests or personal relationships that could have appeared to influence the work reported in this paper.

Data availability

Data will be made available on request.

Acknowledgements

This work was supported by the UK Engineering and Physical Sciences Research Council (EPSRC) grant EP/T022825/1 and EP/T023112/1. The funding sources are for the NetZero GeoRDIE (Net Zero Geothermal Research for District Infrastructure Engineering) and INTEGRATE (Integrating seasoNal Thermal storagE with multiple enerGy souRces to decArobonise Thermal Energy) projects, respectively. For the purpose of open access, the author has applied a Creative Commons Attribution (CC BY) licence to any Author Accepted Manuscript version arising from this submission. We would also like to thank two reviewers for their constructive comments that helped to improve the paper.

References

[1] M.M. Abdelhafiz, L.A. Hegele Jr, J.F. Oppelt, Temperature modeling for wellbore circulation and shut-in with application in vertical geothermal wells, Journal of Petroleum Science and Engineering 204 (2021) 108660.
[2] G. Akhmetova, I. Panfilova, S. Bourlange, A. Pereira, Simulation of wellbore temperature and heat loss in production well in geothermal site, Energy Sources, Part a: Recovery, Utilization, and Environmental Effects 45 (2) (2023) 6262–6273.
[3] R. Al-Khoury, P.G. Bonnier, R.B.J. Brinkgreve, Efficient finite element formulation for geothermal heating systems. Part I: Steady state, International Journal for Numerical Methods in Engineering 63 (7) (2005) 988–1013.
[4] R. Al-Khoury, P.G. Bonnier, Efficient finite element formulation for geothermal heating systems. Part II: transient, International Journal for Numerical Methods in Engineering 67 (5) (2006) 725–745.
[5] D. Banks, An introduction to thermogeology: ground source heating and cooling, John Wiley & Sons, 2012.
[6] C.S. Brown, N.J. Cassidy, S.S. Egan, D. Griffiths, A sensitivity analysis of a single extraction well from deep geothermal aquifers in the Cheshire Basin, UK, Quarterly Journal of Engineering Geology and Hydrogeology 55 (3) (2022).
[7] C.S. Brown, N.J. Cassidy, S.S. Egan, D. Griffiths, Thermal and economic analysis of heat exchangers as part of a geothermal district heating scheme in the cheshire basin, UK. Energies 15 (6) (2022) 1983.
[8] C.S. Brown, L. Howell, Unlocking deep geothermal energy in the UK using borehole heat exchangers, Geology Today 39 (2) (2023) 67–71.
[9] C.S. Brown, H. Doran, I. Kolo, D. Banks, G. Falcone, Investigating the Influence of Groundwater Flow and Charge Cycle Duration on Deep Borehole Heat Exchangers for Heat Extraction and Borehole Thermal Energy Storage, Energies 16 (6) (2023) 2677.
[10] C.S. Brown, I. Kolo, G. Falcone, D. Banks, Investigating scalability of deep borehole heat exchangers: Numerical modelling of arrays with varied modes of operation, Renewable Energy 202 (2023) 442–452.
[11] C. Chen, H. Shao, D. Naumov, Y. Kong, K. Tu, O. Kolditz, Numerical investigation on the performance, sustainability, and efficiency of the deep borehole heat exchanger system for building heating, Geothermal Energy 7 (2019) 1–26.
[12] C. Chen, W. Cai, D. Naumov, K. Tu, H. Zhou, Y. Zhang, O. Kolditz, H. Shao, Numerical investigation on the capacity and efficiency of a deep enhanced U-tube

borehole heat exchanger system for building heating, Renewable Energy 169 (2021) 557–572.
[13] Chen, C. and Shao, H., 2023. Wellbore heat transport – EUBHE. Accessed on 11/4/23 from https://www.opengeosys.org/docs/benchmarks/heat-transport-bhe/pipe_flow_ebhe/.
[14] H.J. Diersch, D. Bauer, W. Heidemann, W. Rühaak, P. Schätzl, Finite element modeling of borehole heat exchanger systems: Part 1, Fundamentals. Computers & Geosciences 37 (8) (2011) 1122–1135.
[15] H.J. Diersch, D. Bauer, W. Heidemann, W. Rühaak, P. Schätzl, Finite element modeling of borehole heat exchanger systems: Part 2, Numerical Simulation. Computers & Geosciences 37 (8) (2011) 1136–1147.
[16] H.J.G. Diersch, FEFLOW: finite element modeling of flow, mass and heat transport in porous and fractured media, Springer Science & Business Media, 2013.
[17] H.R. Doran, T. Renaud, G. Falcone, L. Pan, P.G. Verdin, Modelling an unconventional closed-loop deep borehole heat exchanger (DBHE): sensitivity analysis on the Newberry volcanic setting, Geothermal Energy 9 (1) (2021) 1–24.
[18] J. Hagoort, Ramey's wellbore heat transmission revisited, SPE Journal 9 (04) (2004) 465–474.
[19] A.R. Hasan, C.S. Kabir, Wellbore heat-transfer modeling and applications, Journal of Petroleum Science and Engineering 86 (2012) 127–136.
[20] S. Huang, J. Li, K. Zhu, J. Dong, Y. Jiang, Thermal recovery characteristics of rock and soil around medium and deep U-type borehole heat exchanger, Applied Thermal Engineering (2023) 120071.
[21] S. Huang, J. Li, K. Zhu, J. Dong, Y. Jiang, Influencing factors analysis for the long-term thermal performance of medium and deep U-type borehole heat exchanger system, Journal of Building Engineering 68 (2023) 106152.
[22] K. Kanev, J. Ikeuchi, S. Kimurat, A. Okajima, Heat loss to the surrounding rock formation from a geothermal wellbore, Geothermics 26 (3) (1997) 329–349.
[23] O. Kolditz, S. Bauer, L. Bilke, N. Böttcher, J.O. Delfs, T. Fischer, U.J. Görke, T. Kalbacher, G. Kosakowski, C.I. McDermott, C.H. Park, OpenGeoSys: an open-source initiative for numerical simulation of thermo-hydro-mechanical/chemical (THM/C) processes in porous media, Environmental Earth Sciences 67 (2012) 589–599.
[24] I. Kolo, R. Sousa, T. Zhang, December. Heat transmission in a geothermal wellbore: modelling and application. In Proceedings of the 19th Australasian Fluid Mechanics Conference, 2014.
[25] I. Kolo, C.S. Brown, G. Falcone, D. Banks, Repurposing a Geothermal Exploration Well as a Deep Borehole Heat Exchanger: Understanding Long-Term Effects of Lithological Layering, Flow Direction, and Circulation Flow Rate, Sustainability 15 (5) (2023) 4140.
[26] K. Kutun, O.I. Tureyen, A. Satman, Temperature Behavior of Geothermal Wells during Production, Injection and Shut-in Operations, Stanford University, Stanford, California, 2014.
[27] G. Li, M. Yang, Y. Meng, Z. Wen, Y. Wang, Z. Yuan, Transient heat transfer models of wellbore and formation systems during the drilling process under well kick conditions in the bottom-hole, Applied Thermal Engineering 93 (2016) 339–347.
[28] J. Majorowicz, S. Wybraniec, New terrestrial heat flow map of Europe after regional paleoclimatic correction application, International Journal of Earth Sciences 100 (4) (2011) 881–887.
[29] B. Moradi, M. Ayoub, M. Awang, Modification of Ramey's model for carbon dioxide injection in the vicinity of critical point, Journal of CO2 Utilization 16 (2016) 218–224.
[30] L. Pan, C.M. Oldenburg, T2Well—an integrated wellbore–reservoir simulator, Computers & Geosciences 65 (2014) 46–55.
[31] L. Pan, B. Freifeld, C. Doughty, S. Zakem, M. Sheu, B. Cutright, T. Terrall, Fully coupled wellbore-reservoir modeling of geothermal heat extraction using CO2 as the working fluid, Geothermics 53 (2015) 100–113.
[32] H.J. Ramey Jr, Wellbore heat transmission, Journal of Petroleum Technology 14 (04) (1962) 427–435.
[33] K.E. Rollin, A simple heat-flow quality function and appraisal of heat-flow measurements and heat-flow estimates from the UK Geothermal Catalogue, Tectonophysics 244 (1–3) (1995) 185–196.
[34] Rosca, M., 2000. Heat transfer in a low enthalpy geothermal well. In *World Geothermal Congress* (pp. 1651-1656).
[35] S. Saeid, R. Al-Khoury, F. Barends, An efficient computational model for deep low-enthalpy geothermal systems, Computers & Geosciences 51 (2013) 400–409.
[36] S. Saeid, R. Al-Khoury, H.M. Nick, M.A. Hicks, A prototype design model for deep low-enthalpy hydrothermal systems, Renewable Energy 77 (2015) 408–422.
[37] A. Satter, Heat losses during flow of steam down a wellbore, Journal of Petroleum Technology 17 (07) (1965) 845–851.
[38] M.A. Sbai, A. Larabi, Analyzing the relationship between doublet lifetime and thermal breakthrough at the Dogger geothermal exploitation site in the Paris basin using a coupled mixed-hybrid finite element model, Geothermics 114 (2023) 102795.
[39] H. Shi, J.A. Holmes, L.J. Durlofsky, K. Aziz, L.R. Diaz, B. Alkaya, G. Oddie, Drift-flux modeling of two-phase flow in wellbores, Spe Journal 10 (01) (2005) 24–33.
[40] H. Shi, G. Wang, C. Lu, Numerical investigation on delaying thermal breakthrough by regulating reinjection fluid path in multi-aquifer geothermal system, Applied Thermal Engineering 221 (2023) 119692.
[41] M.M. Tantuoyir, Heat Transfer Modeling and Simulation in Geothermal Wells, University of Stavanger, Norway), 2018. Master's thesis,.
[42] A.P. Wardana, N.M. Saptadji, D.T. Maulana, Study of The Heat Loss Effect in Geothermal Steam Production Well, IOP Conference Series: Earth and Environmental Science Vol. 732, No. 1 (2021).
[43] M. Yang, X. Zhao, Y. Meng, G. Li, L. Zhang, H. Xu, D. Tang, Determination of transient temperature distribution inside a wellbore considering drill string assembly and casing program, Applied Thermal Engineering 118 (2017) 299–314.
[44] P.L. Younger, D.A. Manning, D. Millward, J.P. Busby, C.R. Jones, J.G. Gluyas, Geothermal exploration in the Fell Sandstone Formation (Mississippian) beneath the city centre of Newcastle upon Tyne, UK: the Newcastle Science Central deep geothermal borehole, Quarterly Journal of Engineering Geology and Hydrogeology 49 (4) (2016) 350–363.
[45] Zarrouk, S.J. and McLean, K., 2019. Geothermal well test analysis: fundamentals, applications and advanced techniques.
[46] Zuber, N. and Findlay, J.A., 1965. Average volumetric concentration in two-phase flow systems.